AGU ADVANCING EARTH AND SPACE SCIENCES

Earth's Future

RESEARCH ARTICLE
10.1029/2024EF004922

The West Pacific Teleconnection Drives the Interannual Variability of Autumn Wildfire Weather in the Western United States After 2000

Shizuo Liu[1], **Shineng Hu**[1], **and Richard Seager**[2]

[1]Division of Earth and Climate Sciences, Nicholas School of the Environment, Duke University, Durham, NC, USA, [2]Lamont Doherty Earth Observatory of Columbia University, Palisades, NY, USA

Key Points:

- The autumn West Pacific (WP) teleconnection shifts eastward after 2000
- Since 2000, the WP has been a major climatic factor to the autumn wildfire activity over the western United States (US)
- The effect of WP on autumn western US wildfires was identified in the observations and verified by atmospheric model experiments

Correspondence to:

S. Liu,
shizuo.liu@duke.edu

Citation:

Liu, S., Hu, S., & Seager, R. (2024). The West Pacific teleconnection drives the interannual variability of autumn wildfire weather in the western United States after 2000. *Earth's Future*, *12*, e2024EF004922. https://doi.org/10.1029/2024EF004922

Received 22 MAY 2024
Accepted 16 OCT 2024

Author Contributions:

Conceptualization: Shizuo Liu
Formal analysis: Shizuo Liu, Shineng Hu, Richard Seager
Funding acquisition: Shineng Hu, Richard Seager
Investigation: Shizuo Liu
Methodology: Shizuo Liu
Writing – original draft: Shizuo Liu
Writing – review & editing: Shizuo Liu, Shineng Hu, Richard Seager

Abstract Wildfires pose a significant threat to human society as severe natural disasters. The western United States (US) is one hotspot that has experienced dramatic influences from autumn wildfires especially after 2000, but what has caused its year-to-year variations remains poorly understood. By analyzing observational and atmospheric reanalysis datasets, we found that the West Pacific (WP) pattern centered in the western North Pacific acted as a major climatic factor to the post-2000 autumn wildfire activity by inducing anomalous high pressure over the western US via teleconnections with increased surface temperature, decreased precipitation, and reduced relative humidity. The WP pattern explains about one-third of the post-2000 years-to-year variance of the western US autumn wildfires. These effects were found to be much weaker in the 1980–1990s, as the active region of WP-associated high pressure was confined to the eastern North Pacific. Such eastward shift of the WP teleconnection pattern and its resultant, enhanced influence on the weather conditions of western US autumn wildfire after 2000 are also captured by the sea surface temperature (SST)-forced atmospheric model simulations with the Community Atmosphere Model version 6 (CAM6). The CAM6 ensemble-mean changes in the WP teleconnection pattern at 2000 is about half of the observed changes, which implies that external radiative forcing and/or SST changes have played an important role in the WP pattern shift. Our results highlight a pressing need to consider the joint impacts of atmospheric internal variability and externally forced climate changes when studying the interannual variations of wildfire activity.

Plain Language Summary In the 21st century, particularly in recent years, wildfires have surged in frequency in the western US during autumn, resulting in severe natural disasters and impacting human society. Despite extensive research on summer wildfires, the causes and mechanisms of autumn wildfires remain less understood. This study utilizes observational analysis and model simulations to elucidate the substantial influence of the WP teleconnection on the western US autumn wildfires in the 21st century, attributed to the eastward shift of the WP teleconnection around 2000. Additionally, our findings demonstrate that the WP teleconnection can account for approximately one-third of the interannual variability in autumn wildfires since 2000.

1. Introduction

Wildfire is a severe natural hazard, capable of rapidly spreading, that can cause extensive damage to the environment, wildlife, human health, and infrastructure (Moritz et al., 2014; Qiu et al., 2024; Radeloff et al., 2018). Previous research primarily emphasized the summer season when wildfires typically break out most frequently. In recent years, climate change has extended the wildfire season in the western US, now encompassing not only summer but also autumn and even December (Goss et al., 2020; Hawkins et al., 2022; Williams et al., 2019; Zou et al., 2021). In November 2018, wildfires in California were severe natural disasters, causing at least 85 deaths and 16.5 billions of dollars in damage, which is one of the costliest wildfire events recorded in the modern era in the US (https://www.fire.ca.gov/our-impact/remembering-the-camp-fire). In fact, autumn has experienced the highest number of wildfire events in the US (https://www.ncei.noaa.gov/access/billions/), while investments in firefighting resources are comparatively less in the autumn than in the summer (Goss et al., 2020). This motivates us to investigate the factors contributing to the autumn wildfires over the western US.

During the past two decades, numerous studies have investigated the various factors contributing to the increased frequency and duration of western US wildfires in summer and attributed the cause to factors such as earlier spring snowmelt (Westerling et al., 2006), reduced precipitation and/or humidity (Holden et al., 2018; Jacobson

et al., 2024), anthropogenic global warming (Abatzoglou & Williams, 2016; Harvey, 2016; Jones et al., 2022; Marlon et al., 2012; Turco et al., 2023; Williams et al., 2019), etc. Although drought induced by human-driven global warming is considered the main factor that leads to a substantial rise in summer wildfires across the western US, atmospheric variability also plays an important role (Diffenbaugh et al., 2021; Zhuang et al., 2021). A previous study found that anthropogenic global warming accounts for two-thirds of the increase in wildfires during the entire fire season, while internal variability contributes to the remaining one-third (Zhuang et al., 2021). Concurrently, most studies primarily concentrated on analyzing the reasons for summer wildfire trends, with comparatively limited literature on the factors contributing to its interannual variability. Jacobson et al. (2022) have shown how interannual variability of burned forest area in California in summer is related to precipitation, temperature, humidity, circulation and vapor pressure deficit anomalies stretching back into the prior winter.

As summer wildfires have attracted much attention recently, there are relatively fewer studies investigating autumn wildfires in the western US and why there have been more frequent outbreaks in recent years. Goss et al. (2020) found that increasing temperature and decreasing precipitation had contributed to increases in likelihood of extreme wildfire conditions in California in autumn over the past four decades. Zou et al. (2021) demonstrated that the reduction of summer Arctic sea ice was a contributing factor to autumn wildfire incidence in the western US. Hawkins et al. (2022) found anthropogenic climate change was exacerbating autumn fire weather extremes, similar to summer. In this study, we delve into the key atmospheric dynamical factors affecting autumn (from September to November) wildfire interannual variability in the western US, which remains not fully understood yet.

The West Pacific (WP) pattern is an important internal atmospheric variability pattern of the climate system over the North Pacific (Linkin & Nigam, 2008), which can significantly influence North American winter hydroclimate (Baxter & Nigam, 2015; Linkin & Nigam, 2008). The North Pacific Oscillation (NPO) is the upper-air geopotential height signature of the WP, also suggested to affect North American winter climate (Rogers, 1981; Sung et al., 2019). Previous studies documented that the winter and summer WP/NPO had shifted eastward in recent decades, thereby intensifying its impact on extreme weather events (Hu et al., 2023; Sung et al., 2019; Tian et al., 2024; Xu & Fan, 2020; Yeh et al., 2018). Based on the previous studies, the eastward shift of the WP/NPO pattern may have been caused by various factors, including the change of the mean state of tropical Pacific SST (Park & An, 2014), the depression of convective activity in the central Pacific (Sung et al., 2019), long-term changes of Arctic sea ice (Hu et al., 2023; Kim et al., 2020; Xu & Fan, 2020), changes in North Atlantic SST (i.e., Atlantic Multidecadal Oscillation) (Aru et al., 2023) or the inherent variability within the system itself. Here, we have found a notable eastward shift of the autumn WP after 2000, which will be described in detail later. This shift may have the potential to influence the occurrence and intensity of wildfires during autumn in the western US by affecting the temperature, precipitation, relative humidity (RH), and vapor pressure deficit (VPD) in the region.

In this study, we will use observational and atmospheric reanalysis datasets, as well as CAM6 Atmospheric Model Intercomparison Project (AMIP) outputs to explore this question. The paper is organized as follows. Section 2 describes data and methods, including observational and simulated data selection as well as analysis methods. Section 3 presents the linkage between WP and western US wildfires in the observation. Section 4 presents the shift of the CAM6 simulated WP pattern and its relationship to western US wildfires. Section 5 discusses the potential explanations for the WP shift. Section 6 summarizes and discusses the results.

2. Data and Methods

2.1. Observational Data

In this study, we first use a new observational database of locations and sizes of individual fires in the western US [Western US MTBS-Interagency (WUMI) wildfire database] (Juang et al., 2022). It is a set of high-resolution maps of large wildfires ($\geq$4.04 km^2) provided by the Monitoring Trends in Burn Severity (MTBS) program (Eidenshink et al., 2007) and wildfires $\geq$1 km^2 from the National Wildfire Coordinating Group (NWCG), and the California Department of Forestry and Fire Protection (CalFire). This fire database consists of 18, 368 western US fire events from 1984 through 2019.

Next, several indices are used in this study in order to integrate the complex interactions between climate drivers and wildfire danger. In this study, we use the Canadian Fire Weather Index (FWI) to represent potential fire danger (Van Wagner, 1987), which has been widely used for the US and Canada (Hawkins et al., 2022; Zou et al., 2021). We use two FWI datasets, one is from gridMET (Abatzoglou, 2013) and the other is an ERA5-based FWI product (Vitolo et al., 2020). GridMET is a dataset of daily high-spatial resolution (~4 km, 1/24th degree) surface meteorological data covering the contiguous US from 1979-yesterday (https://www.climatologylab.org/gridmet.html). It integrates the spatial characteristics of gridded climate data from Parameter-elevation Regressions on Independent Slopes Model (PRISM, Daly et al., 2008) and temporal attributes of gridded climate data from the North American Land Data Assimilation System Phase 2 (NLDAS-2, Mitchell et al., 2004). The ERA5-based FWI product is provided by the Copernicus Emergency Management Service, computed with meteorological fields from the ERA5 reanalysis (https://cds.climate.copernicus.eu/cdsapp#!/dataset/cems-fire-historical?tab%20=form), with a 0.25° spatial and daily temporal grid, covering the period from 1 January 1979 to 31 December 2022.

Besides these two FWI datasets, we also use maximum temperature (T_{max}), precipitation accumulation (Pr) and RH from gridMET, and 500 hPa geopotential height (Z500) from ERA5 (Hersbach et al., 2020). The WP index comes from the Climate Prediction Center (CPC) (https://psl.noaa.gov/data/correlation/wp.data). The CPC utilizes the rotated principal component analysis (RPCA) method described by Barnston and Livezey (1987) to calculate the WP index. WP is defined as the fourth RPCA mode of the Z500 anomalies. The teleconnection patterns in the RPCA approach are identified based on the entire flow field over the Northern Hemisphere, and not just from height anomalies at select locations, so it can get better continuity of the time series and robust patterns. VPD is calculated from maximum temperature and relative humidity (Zhuang et al., 2021) as follows:

$$e_s = 611.2 * \exp\left(17.76 * \frac{T_{max} - 273.15}{T_{max} - 29.65}\right) \quad (1)$$

$$VPD = e_s(1 - RH) \quad (2)$$

where T_{max} is in K, RH is expressed as a fraction and e_s is the saturated vapor pressure in Pa.

2.2. The Community Atmosphere Model Version 6 (CAM6) Atmospheric Model Intercomparison Project (AMIP) Experiments

We use the prescribed SST global Atmospheric Model Intercomparison Project (AMIP) ensembles forced with observational SST and sea ice with CAM6 that are performed by NCAR (https://www.earthsystemgrid.org/dataset/ucar.cgd.cesm2.cam6.prescribed_sst_amip.goga.all_years.atm.proc.monthly_ave.html). The CAM6 runs have a horizontal resolution of 1.25° longitude by 0.9° latitude and a total of 10 ensemble members. We focus on 1979–2021 in CAM6 AMIP experiments due to a limited time span from 1850 to 2021. Similar to the observation, an RPCA analysis is applied to the CAM6 Z500 for each model for the entire Northern Hemisphere to get the WP teleconnection (Li et al., 2020). We also used CAM6-simulated T_{max}, Pr and RH, along with VPD calculated by Formulas 1 and 2. Given the complexity of FWI calculations and the comprehensive characterization of fire weather conditions by VPD (Zhuang et al., 2021), we opted not to compute CAM6 FWI in this article.

2.3. Statistical Significance Test

A linear regression analysis is conducted to examine the statistical relationships between year-to-year variations of the WP and other variables at each grid point for these two periods. In CAM6, linear regressions are calculated for each individual run, and then the multi-run mean is obtained by averaging the regression patterns. Subsequently, the significance levels of regression in observations and model results, and later minus earlier regressions in the model use the two-tailed Student's t test (Wilks, 2006). In this study, we used a 90% confidence level. For the model results:

$$t = \frac{\overline{X}}{\sigma/\sqrt{N}} \quad (3)$$

where $\overline{X}$ denotes the ensemble mean regression or the later minus earlier regressions in CAM6 AMIP experiment. σ represents the standard deviation of the anomalies of variables among CAM6. N is the number of the runs.

2.4. Dynamic Diagnostic Methods

Wave activity flux (WAF) is used to study the propagation of Rossby wave. In this study, the WAF formula proposed by Plumb (1985) is used as a powerful diagnostic tool of the three-dimensional propagation of Rossby waves. The horizontal component of Plumb flux is expressed as follows:

$$F_{\lambda} = \frac{p}{2a^2 \cos \varnothing}\left[\left(\frac{\partial \psi'}{\partial \lambda}\right)^2 - \psi' \frac{\partial^2 \psi'}{\partial \lambda^2}\right] \tag{4}$$

$$F_{\varnothing} = -\frac{P}{2a^2}\left(\frac{\partial \psi'}{\partial \lambda}\frac{\partial \psi'}{\partial \varnothing} - \psi' \frac{\partial^2 \psi'}{\partial \lambda \partial \varnothing}\right) \tag{5}$$

where p is the pressure level, a is the Earth's radius, λ and ϕ are longitude and latitude, respectively, and ψ' represents the deviation of stream function from its zonal mean value. For steady flows over reasonably long periods, such as the seasonal mean, Plumb flux is parallel to the group velocity of the stationary waves and its divergence (convergence) is associated with their source (sink) (Plumb, 1985).

3. Observational Impacts of WP on Autumn Western US Wildfires

The WP pattern is one of the dominant teleconnections that control the climate variability of the western US (Linkin & Nigam, 2008; Sung et al., 2019). Through analyzing a recently published wildfire database consisting of 18,368 wildfire events across the western US (the domain is 32°N–50°N, 125°W–110°W) from 1984 to 2019 (Juang et al., 2022), we found a significant correlation between the autumn WP index and the forest wildfire burned area in the western US from 2000 to 2019, with a correlation coefficient of 0.55 ($p < 0.01$). However, the correlation coefficient between the two was lower at only −0.09 during 1984–1999. To test the robustness of these results, we repeat the correlation analysis using two widely used FWI datasets. Similarly, we have identified a statistically significant correlation between the WP index and the FWI for both gridMET ($r = 0.61, p < 0.01$) and ERA5 ($r = 0.56, p < 0.01$) since 2000, but not before 2000 (Figures 1b and 1c). Those changes of the WP-wildfire correlations were accompanied by the changes of the characteristics of the WP index in both its dominant frequency and variance (Figure 1d). The spectral power of WP during 1979–1999 is almost evenly distributed across different frequencies, resembling white noise, but during 2000–2022, has a preferred period around 3 years. The variance of WP increased from 0.39 during 1979–1999 to 0.44 during 2000–2022. Since the autumn wildfire burned area (represented by WUMI index) and the general fire intensity potential (represented by FWI index) over the western US are both significantly correlated with WP in the post-2000, this demonstrates that the WP pattern plays a robust role in influencing the interannual variability of autumn western US wildfires in the 21st century. Given that the correlation coefficient between the WP and the WUMI burned area is 0.55 and the correlation coefficient between the WP and the FWI reaches 0.61, the WP index can explain 31%–37% (about one third) of the interannual variability of autumn wildfires in the western US after 2000.

Why did the correlation coefficient between the WP index and forest wildfires in the western US begin to rise after 2000? In short, the enhanced influence of the WP pattern on the western US autumn wildfire might be linked to the eastward shift of the WP pattern in autumn (Figures 2b and 2d). More specifically, the center of the North Pacific dipole pattern and the anomalous cyclonic circulation over the western North America both exhibit a significant eastward shift after 2000. The difference in the regression of Z500 onto the WP index between the latter period and the earlier period indicates that changes are prominent over the western North Pacific, central-eastern North Pacific and western North America (Figure 2f). This finding is consistent with previous studies that have similarly suggested an eastward shift of the NPO/WP pattern but for the winter season (Sung et al., 2019; Xu & Fan, 2020; Yeh et al., 2018). The cause of the eastward shift of the WP pattern is out of scope of this study, but some speculations are provided in Section 5.

The eastward shift of the WP pattern results in a ridge of high pressure in the western US (Figure 2d), which promote subsidence with warming, a clear sky and fewer clouds, facilitating radiative warming and collectively

10.1029/2024EF004922

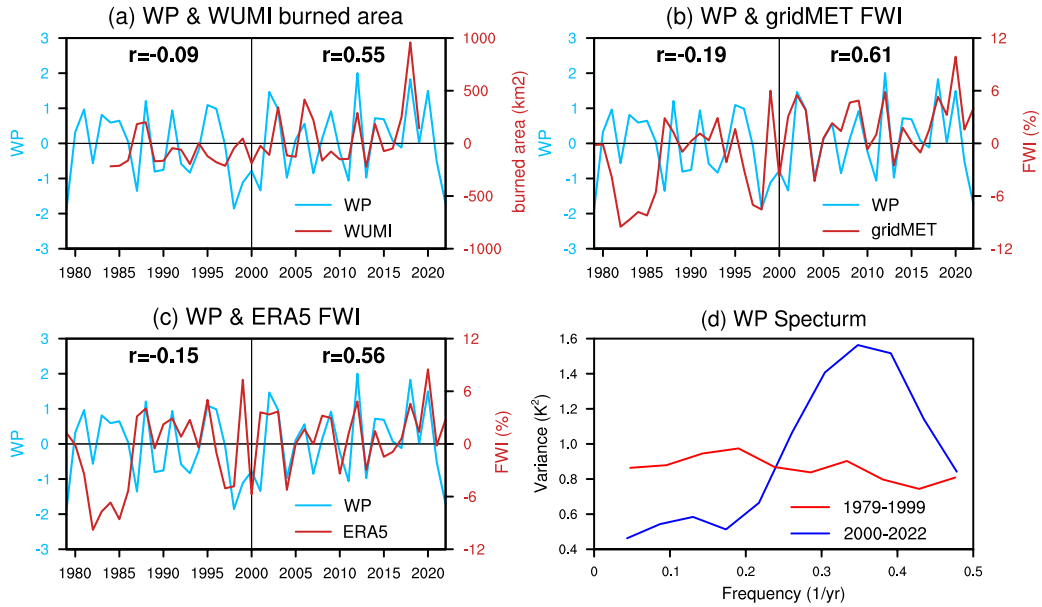

Figure 1. The comparisons of autumn WP index (negative phase, blue curve) from 1979 to 2022 and three western US wildfire indices: the average of western US burned area (WUMI, red curve, unit: km^2) from 1984 to 2019 (a), western US gridMET FWI index (red curve, unit: %) from 1979 to 2022 (b), western US ERA5 FWI index (red curve, unit: %) from 1979 to 2022 (c). The correlation coefficient (r) reaches 0.55 for WUMI and WP, 0.61 for gridMET FWI and WP, and 0.56 for ERA5 FWI and WP in post-2000, statistically significant at the 99% confidence level. The wildfire indices are calculated over the domain: 32°N–50°N and 125°W–110°W. (d) The spectral variance density (*Y*-Axis) versus frequency (*X*-Axis) for 1979–1999 WP (red curve) and 2000–2022 WP (blue curve), respectively.

contributing to a rise in temperature (Wendler et al., 2011) (Figure 3b). Northwesterly flow under the eastern flank of the ridge and the western flank of the low centered between the Great Lakes and Hudson Bay will promote descending air and reduce both precipitation and relative humidity across the western US (Figures 3d and 3f). A significant warming combined with a reduced relative humidity lead to an increased VPD (Figure 3h), which enhances the risk of large wildfires over the western US in autumn (Figures 2c and 2d) (Seager et al., 2015). In contrast, before 2000 the WP is westward displaced over the North Pacific leading to only weak influences on temperature, precipitation, relative humidity, and VPD in the western US (Figure 3) and hardly affecting autumn western US wildfires (Figures 2a and 2b). It is worth noting that, although a correlation between the autumn WP index and the northern or southern US wildfire exists (Figures 2a and 2d), we did not focus on the connections in these regions due to the relatively low frequency of autumn wildfires there.

The green asterisk in Figures 2c and 2d correspond to the site of the Camp Fire in November 2018, the deadliest and most destructive wildfire in California's history (California Department of Finance, 2019). This region is in the center of the region where the significant WP-wildfire relationship is identified (Figures 2c and 2d), suggesting a potential influence of the WP pattern on the occurrence of this exceptionally severe autumn wildfire event in California. Consistently, the regressions of FWI against the WP index (Figures 2c and 2d) show a similar spatial pattern to the change in the annual area burned by fires over the western US between 1984–2001 and 2002–2020 as illustrated in the US Environmental Protection Agency (https://www.epa.gov/climate-indicators/climate-change-indicators-wildfires, their Figure 5). This indicates that in addition to increasing wildfire risk, the WP pattern also seems to be partly associated with the expansion of wildfire burned areas after 2000. However, since the WP index does not have an obvious increasing trend, the multidecadal increasing trend of autumn wildfire activity may be more due to the late 1990s PDO shift (Seager et al., 2023), global warming effect (Abatzoglou & Williams, 2016; Goss et al., 2020) or the increased expansion of human settlements into forested areas (Balch et al., 2017; Hantson et al., 2022). In this study, our primary focus instead lies on examining the interannual variability of the autumn wildfires in the western US and its driving factors.

To validate the robustness of our results, we have also used another approach to compute the WP index for comparison. As the Pacific/North American (PNA) pattern is the dominant mode of atmospheric variability in the

10.1029/2024EF004922

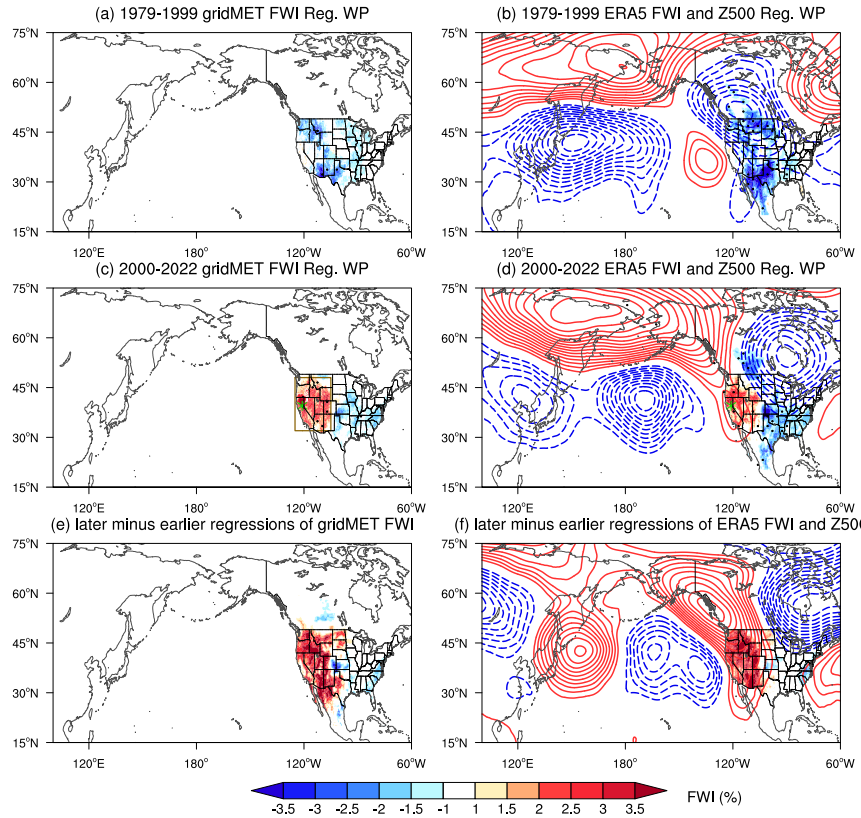

Figure 2. The regressions of autumn gridMET (a), (c) and ERA5 (b), (d) FWI and Z500 against the normalized negative WP index over 1979–1999 (top row) and 2000–2022 (second row), respectively (e), (f) Later minus earlier regressions of gridMET FWI (e), and ERA5 FWI and Z500 (f). The green asterisks in c and d correspond to the site of the Camp Fire. Stippled areas in (a)–(d) denote the regressions of FWI significant at the 90% confidence level based on a two-sided Student's *t* test. Contour intervals are at 2 m in (b) and (d). The orange box in (c) is the domain (32°N–50°N and 125°W–110°W) which is used to calculate the wildfire indices in Figure 1. The zero contour is suppressed in all plots.

North Pacific, we first remove its influence from the 500 mb geopotential height variations in 1979–2022 through an EOF analysis. Then we conduct the EOF analysis again on the residual 500°Nmb geopotential height over the North Pacific region (20°N–70°N, 120°E−120°W) for the two periods 1979–1999 and 2000–2022, separately. The dominant mode of the residual 500 mb geopotential height is expected to be the WP pattern. The identified dominant patterns in the two periods (Figure 4) look similar to Figures 2b and 2d overall with spatial correlation coefficients of 0.87 and 0.93, respectively. The difference of the WP between the two periods (i.e., 2000–2022 minus 1979–1999) also shows a similar pattern to Figure 2f, with a spatial correlation coefficient of 0.78. These results suggest that the eastward shift of the WP pattern is a robust phenomenon and is insensitive to how the WP index is defined.

4. Simulated Impacts of WP by CAM6 AMIP Experiment

To better understand the observed eastward shift of the WP pattern and its influence on the western US autumn wildfire weather conditions, we conduct similar analysis but for 10 AMIP ensemble simulations with the CAM6 model (see Data and methods). To quantitatively evaluate the performance of CAM6 in capturing the spatial structure of WP, we calculate the WP spatial pattern for each model over 1979 to 2021 (Figure 5). The results indicate that CAM6 can reasonably simulate the observed WP pattern, with a spatial correlation ranging from 0.66 to 0.93 over the North Pacific sector. The multi-member mean of the WP pattern exhibits an even higher spatial correlation with the observed WP pattern ($r = 0.94$).

The average WP patterns across the CAM6 AMIP simulations in the two periods are shown in Figures 6a and 6b, which exhibit similar spatial patterns to the observations (Figures 2b and 2d) with a spatial correlation coefficient

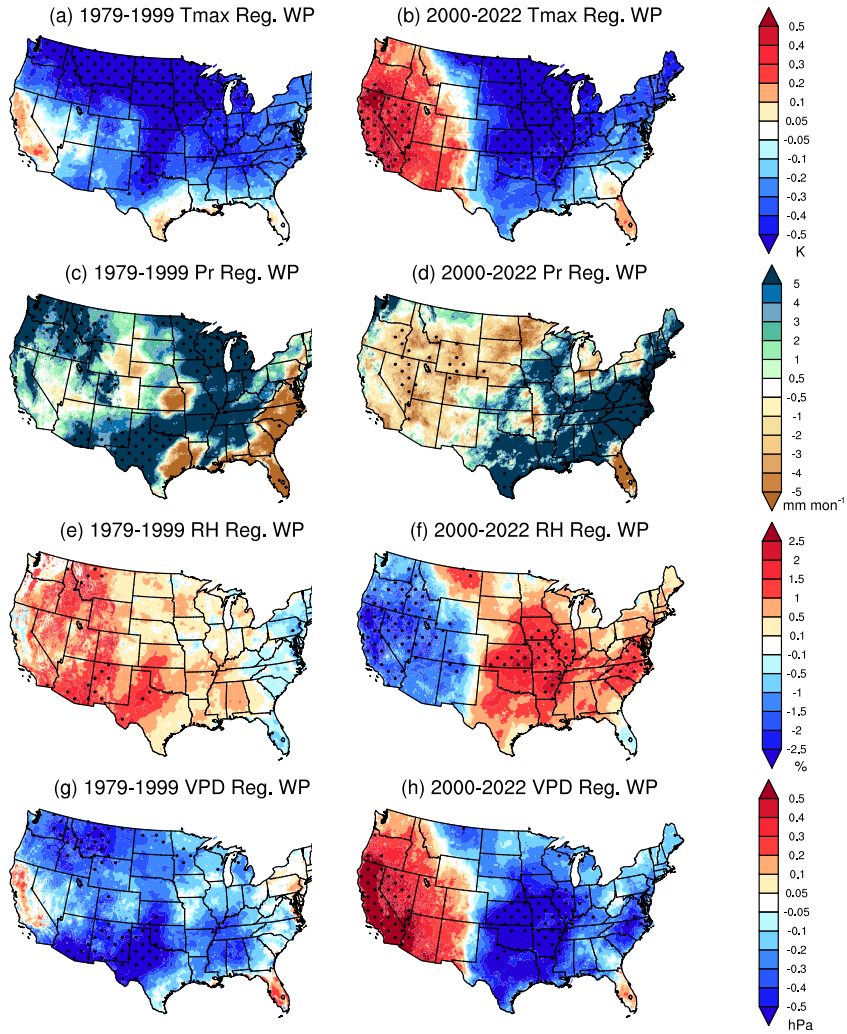

Figure 3. The regression of autumn gridMET T_{max}, Pr, RH and VPD against the normalized negative WP index over 1979–1999 (left column) and 2000–2022 (right column), respectively. Stippled areas in denote values significant at the 90% confidence level based on a two-sided Student's *t* test.

of 0.83 for the pre-2000 period and 0.94 for the post-2000 period. A prominent eastward shift in the North Pacific circulation patterns is identified, although the zonal shift seems to be smaller than observed. The difference of WP pattern (i.e., 2000–2021 WP minus 1979–1999 WP) in CAM6 shows a similar spatial pattern to the observations with positive Z500 anomalies over the western North America and negative Z500 anomaly on its west (Figure 6c; *cf.* Figure 2f). However, the negative anomaly in the eastern North Pacific lies farther north than the observation, whereas the positive anomaly in the western US is situated farther south, and the Z500 anomalies over Asia and the western Pacific are also different. The maximum intensity of the simulated ensemble-mean changes in Z500 over the western US is 5 m (Figure 6c). In contrast, the observed anomalies in this area reach a maximum value of 10–12 m (Figure 2f). Thus, the intensity of these simulated, ensemble-mean changes of Z500 over the western US is approximately half that observed (Figure 2f), which points to a potential role of atmospheric internal variability in the observed WP shift or a potential model bias. Our further investigation on the model ensemble members suggests that 5 out of 10 simulations exhibit a WP teleconnection shift with a similar amplitude as the observed shift.

Next, our analysis will focus on the specific impacts of the shift of the WP on the western US autumn wildfires in CAM6. In contrast to the period over 1979–1999, the intensified anticyclonic circulation over the western US, associated with the negative WP pattern in CAM6, results in an increased temperature in the entire western US after 2000 (Figure 7b). Meanwhile, precipitation and relative humidity decrease in the northwest and southeast

10.1029/2024EF004922

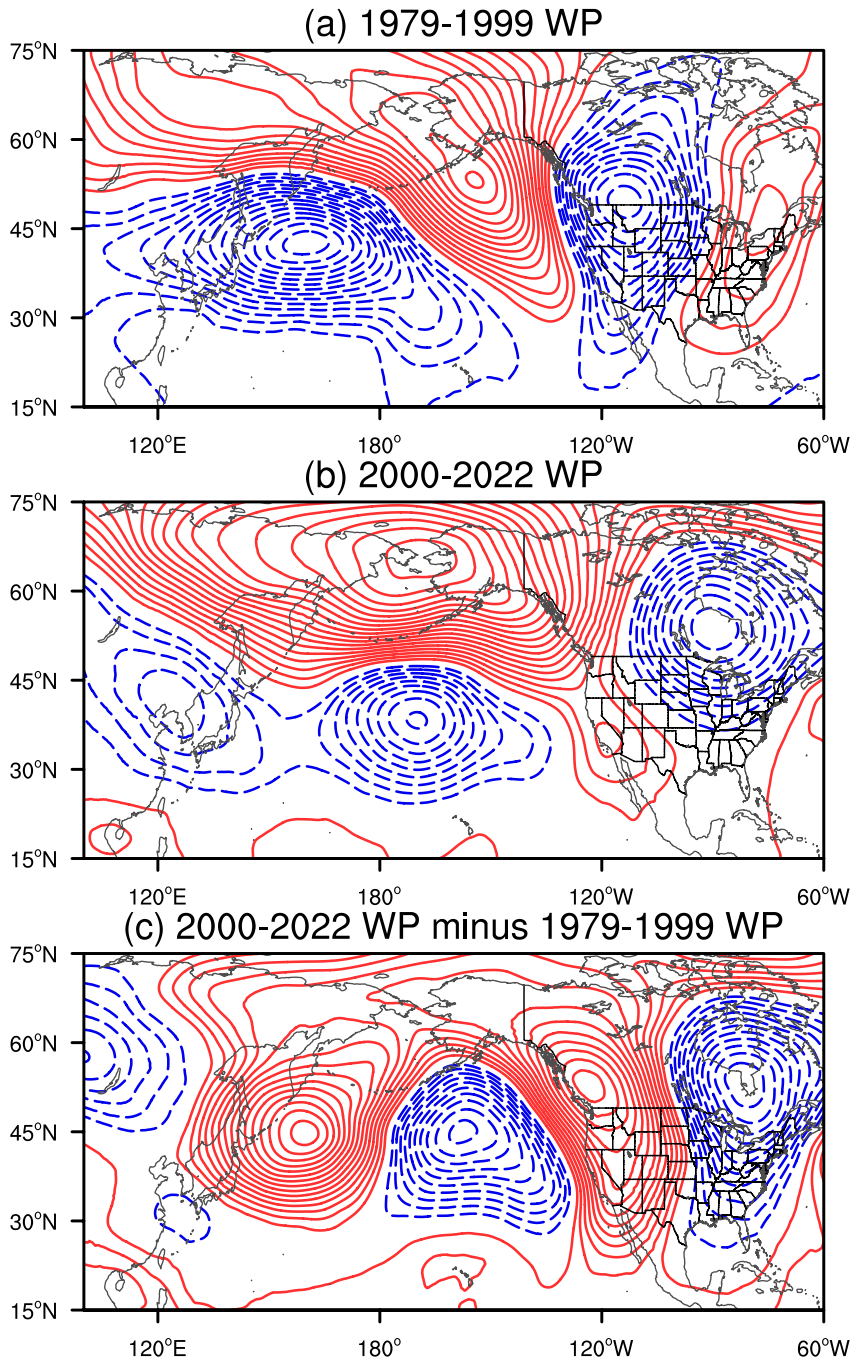

Figure 4. The negative WP patterns over 1979–1999 (a) and 2000–2022 (b), separately. The contours are Z500 anomalies and the intervals are at 2 m. The WP patterns here are obtained by performing EOF on Pacific/North American (PNA)-removed residual heights and for two time periods separately. The zero contour is suppressed in all plots.

regions of the western US. Consequently, these changes lead to an increased VPD across the western US (Figure 7k) and thus promote favorable conditions for wildfires. However, the warmer temperatures and rising VPD are primarily limited to the northwestern and central western regions of the US, slightly northward relative to the observed anomaly. This difference is likely attributed to the positive Z500 anomalies in the multi-run mean WP not extending as far southward as observed after 2000. Before 2000, the westward displacement of the WP pattern results in an increased precipitation and relative humidity over California, ultimately contributing to the decrease in VPD. Finally, comparing later and earlier regressions, it is evident that the eastward shift of the WP

10.1029/2024EF004922

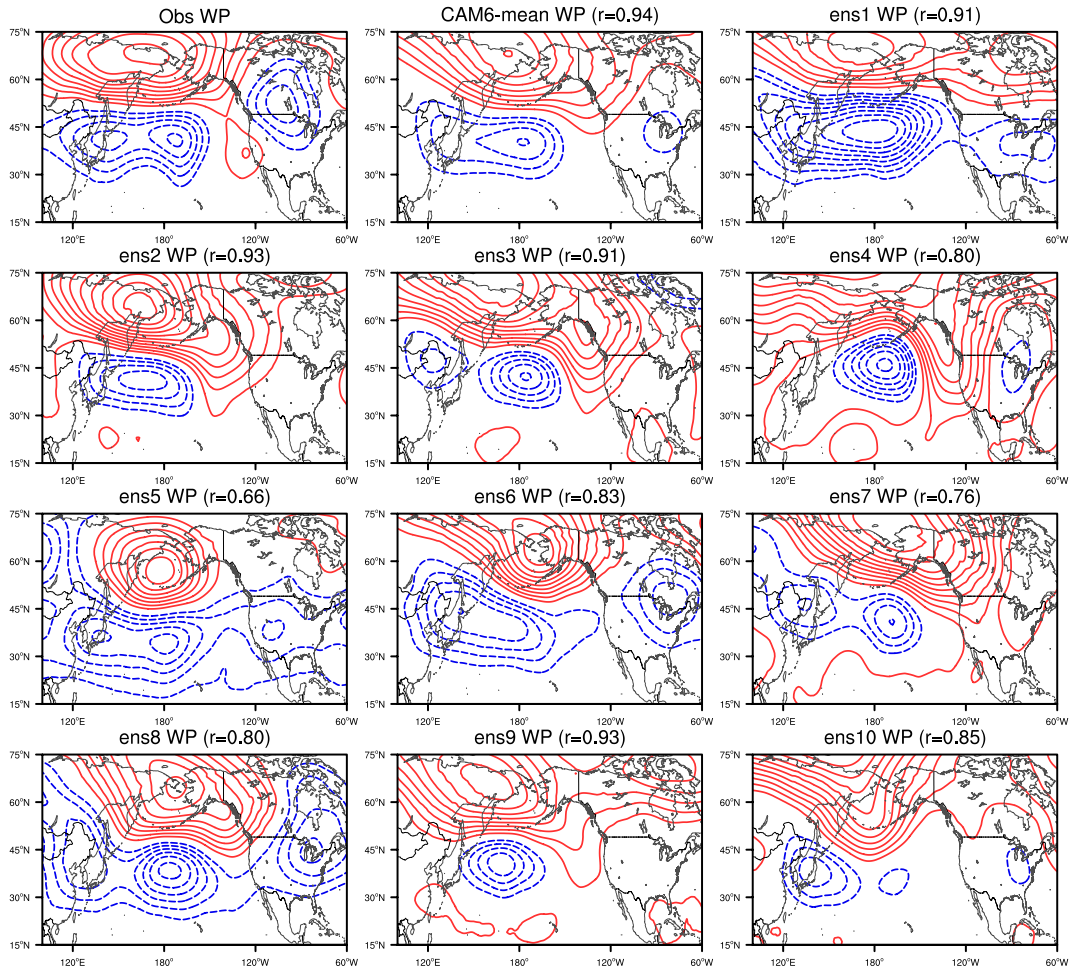

Figure 5. Negative WP spatial patterns for the observations over 1979–2022, the multi-run mean of CAM6 AMIP experiments and each run over 1979–2021, respectively. The contours are Z500 anomalies and the intervals are at 3 m. The values in brackets indicating the spatial correlation coefficient between its spatial pattern and the observed WP over the North-Pacific sector (20°N–70°N, 120°E−120°W). The zero contour is suppressed in all plots.

induces an increased temperature, a decreased precipitation, a decreased relative humidity, and an enhanced VPD across the entire western region (Figures 7c–7i and 7l), consistent with the observed changes.

5. WP Related Rossby Wave Flux in Observation and CAM6

In this section, we attempt to further explore the potential dynamical mechanisms behind the shift of the WP pattern after 2000. Previous studies emphasized stationary wave activities in understanding circulation pattern shifts (Han et al., 2023; Liu et al., 2020). In this study, we employ the wave activity flux (WAF), calculated with Plumb's formulation (Plumb, 1985), as an indicator of the propagation of stationary Rossby waves, and analyzed its pattern associated with the negative WP index for the two periods in the observation and CAM6 (Figure 8).

Before 2000, in the observations, a wave train is initiated at the North Pacific jet entrance, propagating eastward along the waveguide of the subtropical jet stream, and gains energy from strong barotropic instability at the North Pacific jet exit (Branstator, 2002), then strengthening in the northeastern of the Pacific and crossing the western North America afterward (Figure 8a). After 2000, the weakening of the jet stream (Figure 9a) resulted in the westward shift of the cyclonic circulation at the entrance of the North Pacific jet (Figure 8c). This shift caused the formation of two branches of Rossby wave trains, one propagating northeastward to Russian Far East and the other propagating southeastward to central tropical Pacific, separately. These two Rossby wave trains then converged and intensified as they moved toward the exit of the North Pacific jet, subsequently spreading further

10.1029/2024EF004922

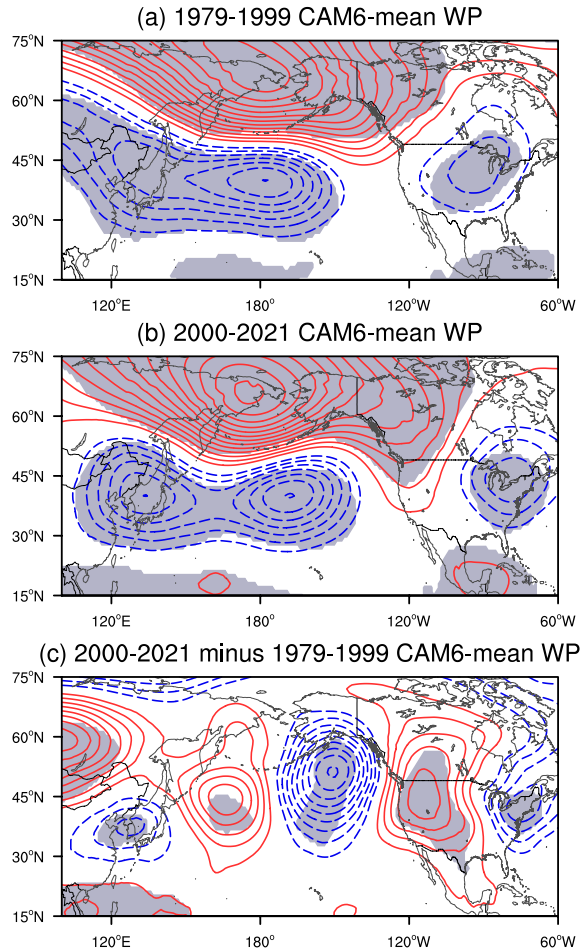

Figure 6. Multi-run mean autumn WP pattern (contours) over 1979–1999 (a) and 2000–2021 (b) from 10 CAM6 AMIP runs. (c) The difference of the multi-run mean WP between 2000–2021 and 1979–1999 (i.e., 2000–2021 minus 1979–1999). The contours are 2 m intervals for (a), (b) and 1 m for (c). Shading areas in denote Z500 anomalies significant at the 90% confidence level based on a two-sided Student's *t* test. The zero contour is suppressed in all plots.

toward North America (Figure 8c). During the post-2000 period, the wave train in CAM6 over the Pacific closely mirrors the observed phenomenon (Figure 8c). Consistently, the changes in the jet stream in CAM6 over the North Pacific around 2000 are comparable with observations (Figure 9). This implies that the interdecadal shift in the global SST and/or the changes of external radiative forcing have contributed to the eastward shift of the WP through both tropical and high-latitude pathways. This is consistent with previous studies attributing winter WP shifts to the changes of Arctic sea ice (Hu et al., 2023) or tropical SST and convection (Sung et al., 2019). A more definitive attribution on the shift of the WP pattern requires further investigations.

6. Summary and Discussion

In recent decades, autumn wildfires became a recurrent concern in the western US, significantly influencing ecosystems, property, infrastructure, livelihoods, and safety in the region (Goss et al., 2020). Despite the severity of these events, previous research on autumn wildfires has been relatively scarce. This study using observational and atmospheric reanalysis datasets and CAM6 AMIP experiment outputs finds that the eastward shift of the WP teleconnection circulation is associated with an influence on the autumn wildfires in the western US after 2000 (Figure 10). This eastward shifted WP pattern contributes to over one-third of the observed interannual autumn wildfire variation in the western US in the 21st century. The eastward shift of the WP teleconnection results in, during its negative phase, a high-pressure ridge in the western US, fostering subsidence with the resultant adiabatic warming and a clear sky with radiative heating. Meanwhile, precipitation and water vapor are reduced.

10.1029/2024EF004922

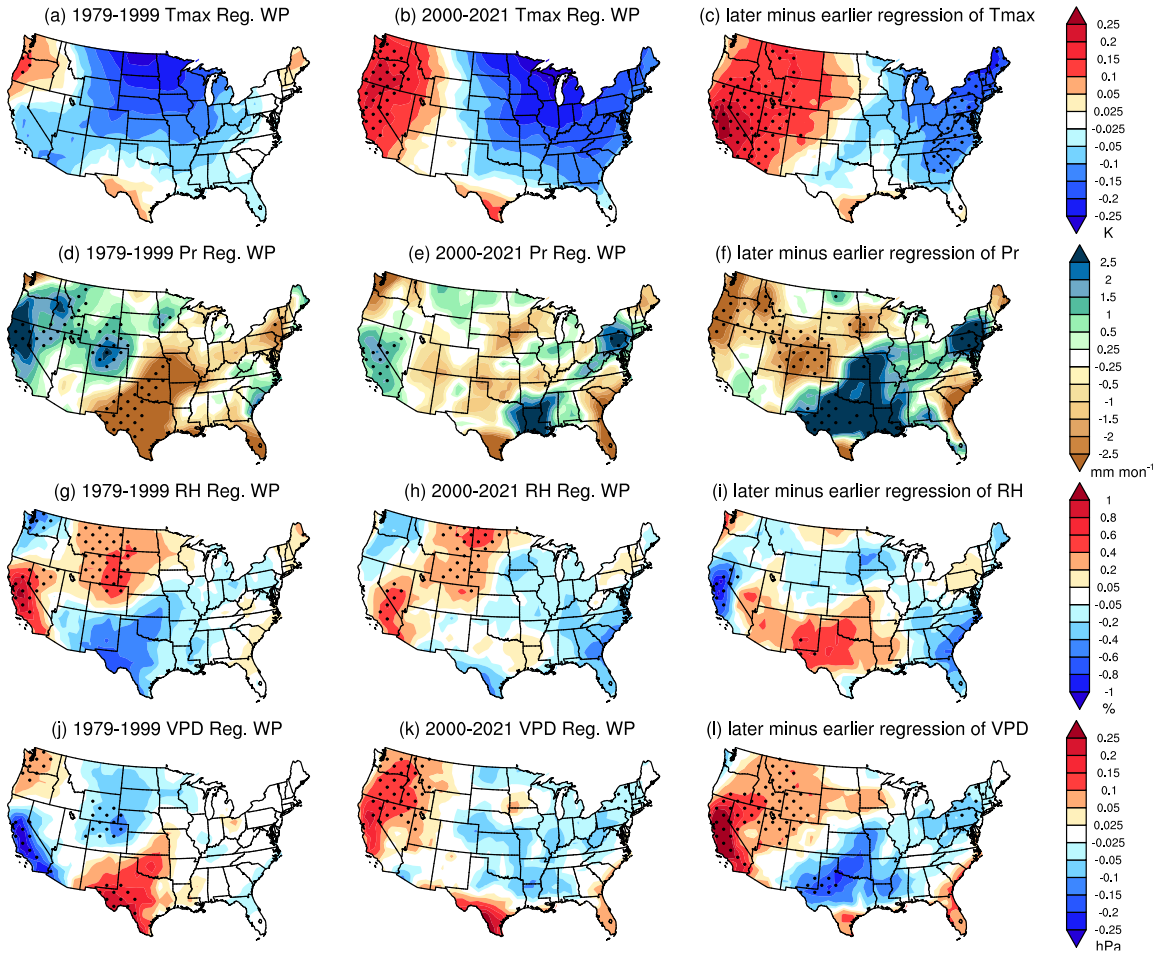

Figure 7. Multi-run mean regressions of T_{max} (first row), Precipitation (second row), RH (third row), VPD (bottom row) against the negative WP index over 1979–1999 (left column) and 2000–2021 (middle column) in CAM6. The right column is the difference of the corresponding regressions between 1979–1999 and 2000–2021 (i.e., 2000–2021 minus 1979–1999). Stippled areas denote values significant at the 90% confidence level based on a two-sided Student's *t* test.

Therefore, the post-2000 negative phase of the WP pattern causes an increased VPD and raises the risk of autumn wildfires. This phenomenon is identified in both observations and SST-forced atmospheric simulations with CAM6, but is more pronounced in the former. Before 2000, the WP pattern could only induce a high-pressure system in the eastern North Pacific and therefore did not play a noticeable role in the autumn wildfires in the western US (Figure 10). The eastward shift of the WP is shown to be associated with the eastward propagation of a wave train, originating in the subtropical jet entrance in the mid-latitude northwest Pacific. After 2000, two branches of Rossby wave trains will propagate from the aforementioned region, one propagating northeastward to the Arctic and the other propagating southwestward to the tropic. They will then intensify at the exit of the North Pacific jet stream. This result suggests that both the Arctic and tropics may exert a certain influence on the shift of the WP (Sung et al., 2019; Xu & Fan, 2020).

It is worth noting that WP, or similarly NPO, is the only climate mode that is significantly correlated with the autumn western US wildfires after 2000, among other climate indices like Niño3.4, PNA, North Atlantic Oscillation (NAO), Pacific Decadal Oscillation (PDO), etc. Furthermore, this mechanism is unique in autumn, not in summer when wildfires are also active. During summer, atmospheric teleconnections are generally weaker, including those connected to fires (Jacobson et al., 2022), leading to a weaker impact on the weather patterns in the western US, and consequently, a weaker influence on wildfires. The WP shift around 2000 also predominantly occurred in autumn and winter, not in summer.

Although CAM6 simulations seem to reveal a discernible link between the decadal variations in global SST or changes of external radiative forcing and the shift of the WP, the simulated intensity of the eastward shift of WP

10.1029/2024EF004922

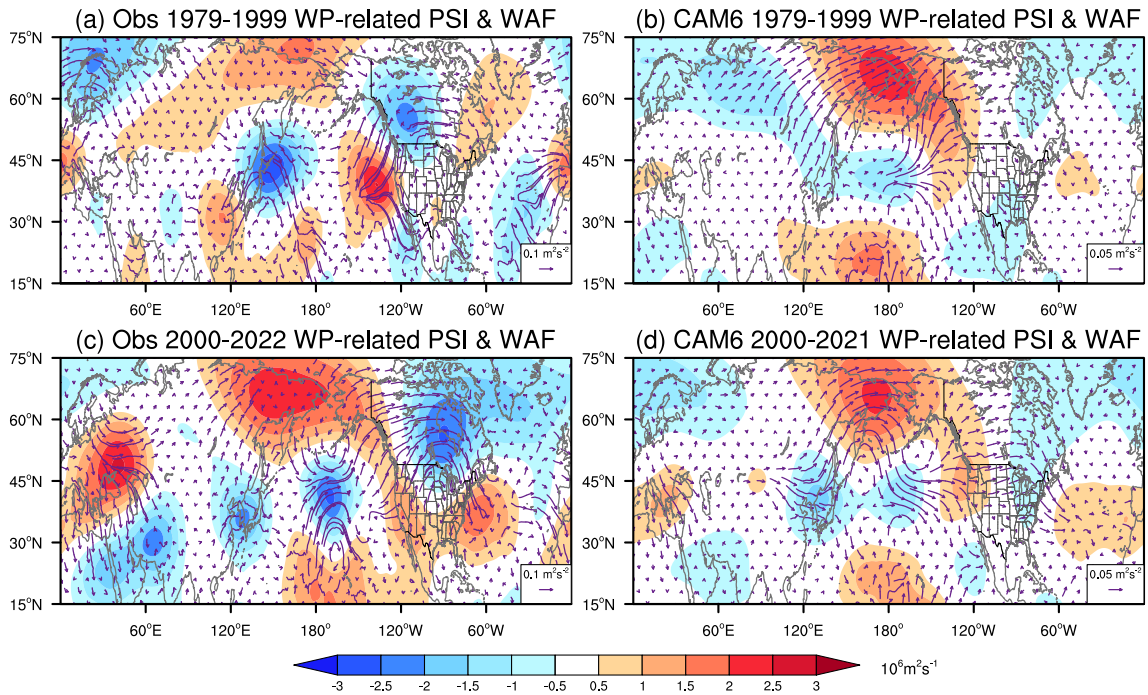

Figure 8. WP related 200 hPa PSI (stream function, shaded area) and Rossby wave flux (WAF, vectors) during Pre-2000 period (a), (b) and Post-2000 period (c), (d) in the observation (left column) and CAM6 (right column).

pattern is considerably weaker than observed, only reaching half that of the observation. Our results suggest that the observed shift in WP around 2000 is attributed to a combination of anthropogenic forcing and natural variability, and both factors need to be considered for a full understanding. We also use Coupled Model Intercomparison Project Phase 6 (CMIP6) for further analysis. The simulated magnitude for the shift of WP is quite weak over western US, only 5% of that in the observations (not shown), although the difference of WP pattern (i.e., 2000–2022 WP minus 1979–1999 WP) in CMIP6 shows a similar spatial pattern to the observations and CAM6 simulations. The weaker WP shift in CMIP6 than in observations or CAM6 simulations could result from that coupled climate models are generally unable to adequately simulate the observed tropical ocean warming pattern that can modulate the teleconnections, as illustrated in previous studies (e.g., Liu & Hu, 2024). In addition, long-term changes in Arctic sea ice or Atlantic sea surface temperature could also contribute to the shift of the WP teleconnection (Aru et al., 2023; Park & An, 2014; Sung et al., 2019; Xu & Fan, 2020; Yeh et al., 2018).

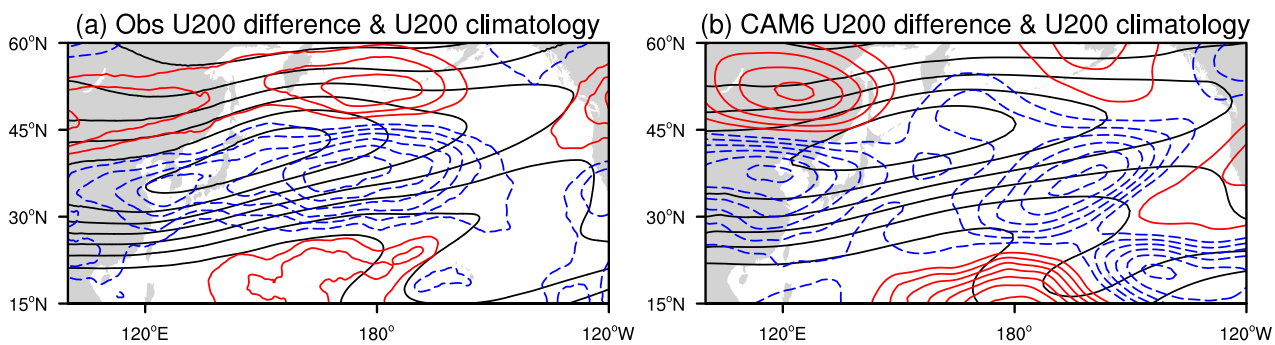

Figure 9. The differences of U200 between the post-2000 period and pre-2000 period in observation (a) and CAM6 (b) (i.e., post-2000 minus pre-2000). The blue dashed and red solid contours represent negative and positive U200 differences with 0.5 m/s intervals for (a) and 0.25 m/s intervals for (b). The black contours in (a) and (b) represent the climatological U200 over the entire period with an interval of 6 m/s. The zero contour is suppressed in all plots.

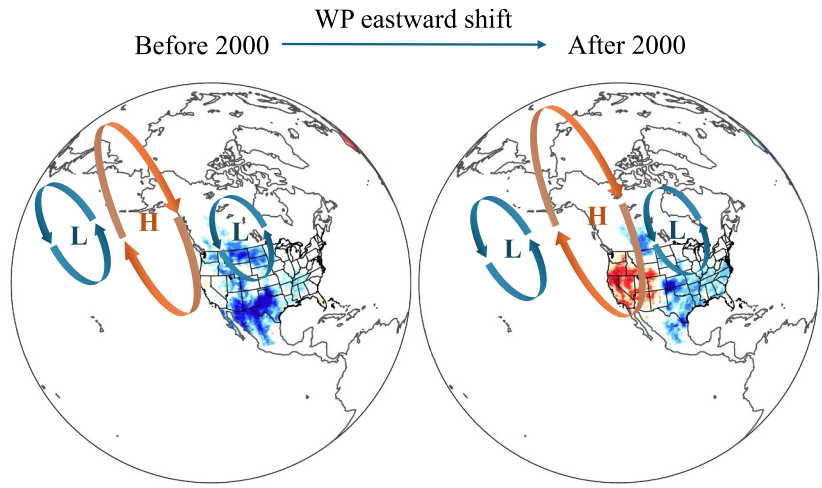

Figure 10. Schematic diagram showing the mechanisms of the influence of the WP on the interannual variability of autumn wildfire weather in the western US, comparing the period after 2000 to that before 2000. After 2000, an anticyclonic circulation associated with the WP emerged over the western US, a weather pattern that increases the risk of autumn wildfires in the region. Before 2000, this circulation was centered over the eastern North Pacific and had little influence on wildfires in the western US. H and L represent the WP-related anticyclonic and cyclonic circulations, respectively. The red (blue) color indicates an increase (decrease) in the risk of autumn wildfires.

Besides the WP teleconnection, many other factors can potentially influence wildfires, including both climatic and non-climatic factors. For non-climate factors, previous studies indicate that since 2000, the rise in wildfires beyond the twentieth century is closely tied to the expansion of human settlement into undeveloped, high-fire-risk areas, which increases fuel exposure to human ignition sources (e.g., Balch et al., 2017; Hantson et al., 2022). Nonetheless, Abatzoglou and Williams (2016) attribute just over half the increase in burned forest area to human-induced climate change. Another previous study shows that the reduction of Arctic sea ice in autumn can also lead to high pressure in the western US through teleconnection, favoring weather conditions conducive to wildfires (Zou et al., 2021). Indeed, we find that the autumn FWI in the western US after 2000 is significantly correlated with the SST ($r = 0.54$) and the sea ice concentration ($r = 0.47$), but its underlying causality and mechanism remain elusive. Thus, the factors influencing the US wildfire weather conditions are likely multifaceted, and the exact mechanisms and their attribution need to be further explored.

Conflict of Interest

The authors declare no conflicts of interest relevant to this study.

Data Availability Statement

The data used in the manuscript are all publicly available for WUMI burned area (Juang & Williams, 2022), gridMET (https://www.northwestknowledge.net/metdata/data/), ERA5-based FWI (Copernicus Climate Change Service, Climate Data Store, 2019), ERA5 (Hersbach et al., 2023a, Hersbach et al., 2023b), WP index (https://psl.noaa.gov/data/correlation/wp.data), CAM6 experiments (https://www.earthsystemgrid.org/dataset/ucar.cgd.cesm2.cam6.prescribed_sst_amip.goga.all_years.atm.proc.monthly_ave.html).

Acknowledgments
This study is supported by the National Aeronautics and Space Administration Award 80NSSC22K1025, National Science Foundation awards AGS-2127684 and AGS-2101214.

References

Abatzoglou, J. T. (2013). Development of gridded surface meteorological data for ecological applications and modelling. *International Journal of Climatology*, *33*(1), 121–131. https://doi.org/10.1002/joc.3413

Abatzoglou, J. T., & Williams, A. P. (2016). Impact of anthropogenic climate change on wildfire across western US forests. *Proceedings of the National Academy of Sciences*, *113*(42), 11770–11775. https://doi.org/10.1073/pnas.1607171113

Aru, H., Chen, W., Chen, S., An, X., Ma, T., & Cai, Q. (2023). Asymmetrical modulation of the relationship between the western pacific pattern and El Niño–southern oscillation by the Atlantic multidecadal oscillation in the boreal winter. *Geophysical Research Letters*, *50*(14), e2023GL103356. https://doi.org/10.1029/2023GL103356

Balch, J. K., Bradley, B. A., Abatzoglou, J. T., Nagy, R. C., Fusco, E. J., & Mahood, A. L. (2017). Human-started wildfires expand the fire niche across the United States. *Proceedings of the National Academy of Sciences*, *114*(11), 2946–2951. https://doi.org/10.1073/pnas.1617394114

Barnston, A. G., & Livezey, R. E. (1987). Classification, seasonality and persistence of low-frequency atmospheric circulation patterns. *Monthly Weather Review*, *115*(6), 1083–1126. https://doi.org/10.1175/1520-0493(1987)115%3C1083:CSAPOL%3E2.0.CO;2

Baxter, S., & Nigam, S. (2015). Key role of the North Pacific Oscillation–west Pacific pattern in generating the extreme 2013/14 North American winter. *Journal of Climate*, *28*(20), 8109–8117. https://doi.org/10.1175/JCLI-D-14-00726.1

Branstator, G. (2002). Circumglobal teleconnections, the jet stream waveguide, and the North Atlantic Oscillation. *Journal of Climate*, *15*(14), 1893–1910. https://doi.org/10.1175/1520-0442(2002)015%3C1893:CTTJSW%3E2.0.CO;2

California Department of Finance. (2019). *California tops 39.9 million residents at new year per new state demographic report*. Data Reflect Fire-Driven Changes to Local Populations, Housing.

Copernicus Climate Change Service, Climate Data Store. (2019). Fire danger indices historical data from the Copernicus emergency management Service. *Copernicus Climate Change Service (C3S) Climate Data Store (CDS)*. [Dataset]. https://doi.org/10.24381/cds.0e89c522

Daly, C., Halbleib, M., Smith, J. I., Gibson, W. P., Doggett, M. K., Taylor, G. H., et al. (2008). Physiographically sensitive mapping of climatological temperature and precipitation across the conterminous United States. *International Journal of Climatology: a Journal of the Royal Meteorological Society*, *28*(15), 2031–2064. https://doi.org/10.1002/joc.1688

Diffenbaugh, N. S., Konings, A. G., & Field, C. B. (2021). Atmospheric variability contributes to increasing wildfire weather but not as much as global warming. *Proceedings of the National Academy of Sciences*, *118*(46), e2117876118. https://doi.org/10.1073/pnas.2117876118

Eidenshink, J., Schwind, B., Brewer, K., Zhu, Z. L., Quayle, B., & Howard, S. (2007). A project for monitoring trends in burn severity. *Fire ecology*, *3*(1), 3–21. https://doi.org/10.4996/fireecology.0301003

Goss, M., Swain, D. L., Abatzoglou, J. T., Sarhadi, A., Kolden, C. A., Williams, A. P., & Diffenbaugh, N. S. (2020). Climate change is increasing the likelihood of extreme autumn wildfire conditions across California. *Environmental Research Letters*, *15*(9), 094016. https://doi.org/10.1088/1748-9326/ab83a7

Han, T., He, S., Zhou, B., Li, S., & Hao, X. (2023). Interdecadal changes in the linkage between North Pacific oscillation during may and northeast China precipitation during mid-summer: The influence of North Atlantic oscillation. *Earth's Future*, *11*(11), e2023EF003754. https://doi.org/10.1029/2023ef003754

Hantson, S., Andela, N., Goulden, M. L., & Randerson, J. T. (2022). Human-ignited fires result in more extreme fire behavior and ecosystem impacts. *Nature Communications*, *13*(1), 2717. https://doi.org/10.1038/s41467-022-30030-2

Harvey, B. J. (2016). Human-caused climate change is now a key driver of forest fire activity in the western United States. *Proceedings of the National Academy of Sciences*, *113*(42), 11649–11650. https://doi.org/10.1073/pnas.1612926113

Hawkins, L. R., Abatzoglou, J. T., Li, S., & Rupp, D. E. (2022). Anthropogenic influence on recent severe autumn fire weather in the west coast of the United States. *Geophysical Research Letters*, *49*(4), e2021GL095496. https://doi.org/10.1029/2021GL095496

Hersbach, H., Bell, B., Berrisford, P., Hirahara, S., Horányi, A., Muñoz-Sabater, J., et al. (2020). The ERA5 global reanalysis. *Quarterly Journal of the Royal Meteorological Society*, *146*(730), 1999–2049. https://doi.org/10.1002/qj.3803

Hersbach, H., Bell, B., Berrisford, P., Hirahara, S., Horányi, A., Muñoz-Sabater, J., et al. (2023a). ERA5 monthly averaged data on single levels from 1940 to present. *Copernicus Climate Change Service (C3S) Climate Data Store (CDS)*. [Dataset]. https://doi.org/10.24381/cds.f17050d7

Hersbach, H., Bell, B., Berrisford, P., Hirahara, S., Horányi, A., Muñoz-Sabater, J., et al. (2023b). ERA5 monthly averaged data on pressure levels from 1940 to present. *Copernicus Climate Change Service (C3S) Climate Data Store (CDS)*. [Dataset]. https://doi.org/10.24381/cds.6860a573

Holden, Z. A., Swanson, A., Luce, C. H., Jolly, W. M., Maneta, M., Oyler, J. W., et al. (2018). Decreasing fire season precipitation increased recent western US forest wildfire activity. *Proceedings of the National Academy of Sciences*, *115*(36), E8349–E8357. https://doi.org/10.1073/pnas.1802316115

Hu, Y., Zhou, B., Han, T., & Li, H. (2023). Enhanced linkage of summer drought in southern China to the North Pacific oscillation since 2000. *Journal of Geophysical Research: Atmospheres*, *128*(4), e2022JD037432. https://doi.org/10.1029/2022JD037432

Jacobson, T. W., Seager, R., Williams, A. P., & Henderson, N. (2022). Climate dynamics preceding summer forest fires in California and the extreme case of 2018. *Journal of Applied Meteorology and Climatology*, *61*(8), 989–1002. https://doi.org/10.1175/JAMC-D-21-0198.1

Jacobson, T. W., Seager, R., Williams, A. P., Simpson, I. R., McKinnon, K. A., & Liu, H. (2024). An unexpected decline in spring atmospheric humidity in the interior Southwestern United States and implications for forest fires. *Journal of Hydrometeorology*, *25*(3), 373–390. https://doi.org/10.1175/JHM-D-23-0121.1

Jones, M. W., Abatzoglou, J. T., Veraverbeke, S., Andela, N., Lasslop, G., Forkel, M., et al. (2022). Global and regional trends and drivers of fire under climate change. *Reviews of Geophysics*, *60*(3), e2020RG000726. https://doi.org/10.1029/2020RG000726

Juang, C., & Williams, P. (2022). Western US MTBS-Interagency (WUMI) wildfire dataset. *Zenodo*. [Dataset]. https://doi.org/10.5061/dryad.sf7m0cg72

Juang, C. S., Williams, A. P., Abatzoglou, J. T., Balch, J. K., Hurteau, M. D., & Moritz, M. A. (2022). Rapid growth of large forest fires drives the exponential response of annual forest-fire area to aridity in the western United States. *Geophysical Research Letters*, *49*(5), e2021GL097131. https://doi.org/10.1029/2021GL097131

Kim, H., Yeh, S. W., An, S. I., Park, J. H., Kim, B. M., & Baek, E. H. (2020). Arctic sea ice loss as a potential trigger for central Pacific El Niño events. *Geophysical Research Letters*, *47*(7), e2020GL087028. https://doi.org/10.1029/2020GL087028

Li, M., Yao, Y., Simmonds, I., Luo, D., Zhong, L., & Chen, X. (2020). Collaborative impact of the NAO and atmospheric blocking on European heatwaves, with a focus on the hot summer of 2018. *Environmental Research Letters*, *15*(11), 114003. https://doi.org/10.1088/1748-9326/aba6ad

Linkin, M. E., & Nigam, S. (2008). The North Pacific Oscillation–west Pacific teleconnection pattern: Mature-phase structure and winter impacts. *Journal of Climate*, *21*(9), 1979–1997. https://doi.org/10.1175/2007JCLI2048.1

Liu, S., & Hu, S. (2024). A 21st century shift in the mechanisms of the early-winter United States snowfall variability. *Environmental Research Letters*, *19*(7), 074021. https://doi.org/10.1088/1748-9326/ad4e4d

Liu, S., Wu, Q., Schroeder, S. R., Yao, Y., Zhang, Y., Wu, T., et al. (2020). Near-global atmospheric responses to observed springtime Tibetan Plateau snow anomalies. *Journal of Climate*, *33*(5), 1691–1706. https://doi.org/10.1175/JCLI-D-19-0229.1

Marlon, J. R., Bartlein, P. J., Gavin, D. G., Long, C. J., Anderson, R. S., Briles, C. E., et al. (2012). Long-term perspective on wildfires in the western USA. *Proceedings of the National Academy of Sciences*, *109*(9), E535–E543. https://doi.org/10.1073/pnas.1112839109

Mitchell, K. E., Lohmann, D., Houser, P. R., Wood, E. F., Schaake, J. C., Robock, A., et al. (2004). The multi-institution North American Land Data Assimilation System (NLDAS): Utilizing multiple GCIP products and partners in a continental distributed hydrological modeling system. *Journal of Geophysical Research*, *109*(D7). https://doi.org/10.1029/2003JD003823

Moritz, M. A., Batllori, E., Bradstock, R. A., Gill, A. M., Handmer, J., Hessburg, P. F., et al. (2014). Learning to coexist with wildfire. *Nature*, *515*(7525), 58–66. https://doi.org/10.1038/nature13946

Park, J. H., & An, S. I. (2014). The impact of tropical western Pacific convection on the North Pacific atmospheric circulation during the boreal winter. *Climate Dynamics*, *43*(7–8), 2227–2238. https://doi.org/10.1007/s00382-013-2047-7

Plumb, R. A. (1985). On the three-dimensional propagation of stationary waves. *Journal of the Atmospheric Sciences*, *42*(3), 217–229. https://doi.org/10.1175/1520-0469(1985)042%3C0217:OTTDPO%3E2.0.CO;2

Qiu, M., Li, J., Gould, C., Jing, R., Kelp, M., Childs, M., et al. (2024). Wildfire smoke exposure and mortality burden in the US under future climate change. https://doi.org/10.31223/X5RQ5C

Radeloff, V. C., Helmers, D. P., Kramer, H. A., Mockrin, M. H., Alexandre, P. M., Bar-Massada, A., et al. (2018). Rapid growth of the US wildland-urban interface raises wildfire risk. *Proceedings of the National Academy of Sciences*, *115*(13), 3314–3319. https://doi.org/10.1073/pnas.1718850115

Rogers, J. C. (1981). The north Pacific oscillation. *Journal of Climatology*, *1*(1), 39–57. https://doi.org/10.1002/joc.3370010106

Seager, R., Hooks, A., Williams, A. P., Cook, B., Nakamura, J., & Henderson, N. (2015). Climatology, variability, and trends in the US vapor pressure deficit, an important fire-related meteorological quantity. *Journal of Applied Meteorology and Climatology*, *54*(6), 1121–1141. https://doi.org/10.1175/JAMC-D-14-0321.1

Seager, R., Ting, M., Alexander, P., Liu, H., Nakamura, J., Li, C., & Newman, M. (2023). Ocean-forcing of cool season precipitation drives ongoing and future decadal drought in southwestern North America. *npj Climate and Atmospheric Science*, *6*(1), 141. https://doi.org/10.1038/s41612-023-00461-9

Sung, M. K., Jang, H. Y., Kim, B. M., Yeh, S. W., Choi, Y. S., & Yoo, C. (2019). Tropical influence on the North Pacific oscillation drives winter extremes in NorthNorth America. *Nature Climate Change*, *9*(5), 413–418. https://doi.org/10.1038/s41558-019-0461-5

Tian, Z., Ding, R., & Zhou, X. (2024). Effect of eastward shift of North Pacific Oscillation on the wind-evaporation-SST feedback. *Climate Dynamics*, *62*(5), 1–10. https://doi.org/10.1007/s00382-023-07061-6

Turco, M., Abatzoglou, J. T., Herrera, S., Zhuang, Y., Jerez, S., Lucas, D. D., et al. (2023). Anthropogenic climate change impacts exacerbate summer forest fires in California. *Proceedings of the National Academy of Sciences*, *120*(25), e2213815120. https://doi.org/10.1073/pnas.2213815120

Van Wagner, C. E. (1987). Development and structure of the Canadian forest fire weather index system (Vol. *35*).

Vitolo, C., Di Giuseppe, F., Barnard, C., Coughlan, R., San-Miguel-Ayanz, J., Libertá, G., & Krzeminski, B. (2020). ERA5-based global meteorological wildfire danger maps. *Scientific Data*, *7*(1), 216. https://doi.org/10.1038/s41597-020-0554-z

Wendler, G., Conner, J., Moore, B., Shulski, M., & Stuefer, M. (2011). Climatology of Alaskan wildfires with special emphasis on the extreme year of 2004. *Theoretical and Applied Climatology*, *104*(3–4), 459–472. F. https://doi.org/10.1007/s00704-010-0357-9

Westerling, A. L., Hidalgo, H. G., Cayan, D. R., & Swetnam, T. W. (2006). Warming and earlier spring increase western US forest wildfire activity. *Science*, *313*(5789), 940–943. https://doi.org/10.1126/science.1128834

Wilks, D. S. (2006). *Statistical methods in the atmospheric sciences* (2nd ed.). Academic Press.

Williams, A. P., Abatzoglou, J. T., Gershunov, A., Guzman-Morales, J., Bishop, D. A., Balch, J. K., & Lettenmaier, D. P. (2019). Observed impacts of anthropogenic climate change on wildfire in California. *Earth's Future*, *7*(8), 892–910. https://doi.org/10.1029/2019EF001210

Xu, Z., & Fan, K. (2020). Prolonged periodicity and eastward shift of the January North Pacific Oscillation since the mid-1990s and its linkage with sea ice anomalies in the Barents Sea. *Journal of Geophysical Research: Atmospheres*, *125*(13), e2020JD032484. https://doi.org/10.1029/2020JD032484

Yeh, S. W., Yi, D. W., Sung, M. K., & Kim, Y. H. (2018). An eastward shift of the North Pacific Oscillation after the mid-1990s and its relationship with ENSO. *Geophysical Research Letters*, *45*(13), 6654–6660. https://doi.org/10.1029/2018GL078671

Zhuang, Y., Fu, R., Santer, B. D., Dickinson, R. E., & Hall, A. (2021). Quantifying contributions of natural variability and anthropogenic forcings on increased fire weather risk over the western United States. *Proceedings of the National Academy of Sciences*, *118*(45), e2111875118. https://doi.org/10.1073/pnas.2111875118

Zou, Y., Rasch, P. J., Wang, H., Xie, Z., & Zhang, R. (2021). Increasing large wildfires over the western United States linked to diminishing sea ice in the Arctic. *Nature Communications*, *12*(1), 6048. https://doi.org/10.1038/s41467-021-26232-9